AGU PUBLICATIONS

JGR

Journal of Geophysical Research: Oceans

RESEARCH ARTICLE

10.1002/2016JC011726

On the long-term stability of the Lofoten Basin Eddy

H. Søiland[1], L. Chafik[2,3], and T. Rossby[4]

[1]Institute of Marine Research and Bjerknes Centre for Climate Research, Bergen, Norway, [2]NOAA/NESDIS Center for Satellite Application and Research, College Park, Maryland, USA, [3]Cooperative Institute for Climate and Satellites, University of Maryland, College Park, Maryland, USA, [4]Graduate School of Oceanography, University of Rhode Island, South Ferry Road, Narragansett, Rhode Island, USA

Key Points:
- Stable, permanent feature of the Lofoten Basin
- Core relative vorticity close to its theoretical extremum, $-f$
- Wanders cyclonically around the deepest part of the Lofoten Basin

Supporting Information:
- Supporting Information S1
- Movie S1

Correspondence to:
H. Søiland,
henrik.soiland@imr.no

Citation:
Søiland, H., L. Chafik, and T. Rossby (2016), On the long-term stability of the Lofoten Basin Eddy, *J. Geophys. Res. Oceans*, *121*, 4438–4449, doi:10.1002/2016JC011726.

Received 16 FEB 2016
Accepted 22 MAY 2016
Accepted article online 2 JUN 2016
Published online 1 JUL 2016
Corrected 25 JUL 2016

This article was corrected on 25 JUL 2016. See the end of the full text for details.

Abstract In recent years, several studies have identified an area of intense anticyclonic activity about 500 km straight west of the Lofoten Islands at 70°N in the northern Norwegian Sea. Now recognized as the coherent Lofoten Basin Eddy (LBE), it is maintained by a supply of anticyclonic eddies that break away from the Norwegian Atlantic Current. Here we show from ship-based surveys of its velocity field that it is quite stable with a central core in solid body rotation ∼1000 m deep, ∼8 km radius, and a relative vorticity close to its theoretical limit $-f$. The surveys also show the LBE typically has a >60 km radius with maximum swirl velocities at 17–20 km radius. From the velocity field, we estimate the dynamic height amplitude at the surface to be about ∼0.21 ± 0.03 dyn. m. Second, altimetry from the last 20 years shows the extremum in sea surface height relative to the surrounding waters to be about the same, 0.2 dyn. m. Third, a float trapped in the LBE for many months reveals a clear cyclonic wandering of the eddy over the deepest parts of the basin. Last, three hydrographic sections from the 1960s show the dynamic height signal to be virtually the same then as it is now. From these observations, we conclude that the LBE is a permanent feature of the Nordic Seas and plays a central role in maintaining the pool of warm water in the western Lofoten Basin.

1. Introduction

The Norwegian Sea comprises two basins, the Norwegian and the Lofoten Basins in the south and north (Figure 1), respectively. Although they both have warm and salty North Atlantic water flowing along their eastern margins, they differ fundamentally in the thermal makeup [*Helland-Hansen and Nansen*, 1909; *Björk et al*., 2001]. The Norwegian Basin is supplied by a warm inflow over the Iceland Faroe Ridge and through the Faroe Shetland Channel. These warm waters flow northward through the Norwegian Basin in the outer and inner branch of the Norwegian Atlantic Current (NwAC) along the eastern margin of the basin [*Orvik and Niiler*, 2002]. These warm currents appear to be rather stable such that there is little leakage of warm water into the western part of the basin [see e.g., *Rossby et al*., 2009a]. As a result, the hydrographic properties of the central and western parts of the Norwegian Basin are principally governed by waters originating in the Iceland Sea to its west and the Greenland Sea farther north with only a thin surface layer with properties influenced by Atlantic Water.

The Lofoten Basin, on the other hand, has a thick layer of Atlantic Water covering the entire basin [*Rossby et al*., 2009a]. In the south east of the basin, a nearly barotropic branch of the NwAC flows along the shelf edge, and a baroclinic branch of the NwAC flows along the Mohn Ridge in the northwest [*Poulain et al*., 1996; *Skagseth et al*., 2004; *Chafik et al*., 2015]. But what really sets the Lofoten Basin apart and makes it so warm is that this inner branch goes unstable where the escarpment becomes exceptionally steep off the Lofoten Islands leading to the frequent shedding of anticyclonic eddies, which then drift toward the deepest part of the basin ∼500 km to the west [*Köhl*, 2007; *Andersson et al*., 2011; *Koszalka et al*., 2011; *Volkov et al*., 2013; *Raj et al*., 2015; *Chafik et al*., 2015]. This continual supply of warm eddies leads to a general deepening of isotherms throughout especially the western half of the Lofoten Basin where it appears that the eddies converge to create and maintain a possibly permanent eddy [*Köhl*, 2007; *Rossby et al*., 2009a; *Volkov et al*., 2013; *Raj et al*., 2015; *Chafik et al*., 2015]. *Köhl* [2007] also refers to two papers by *Ivanov and Korablev* [1995a,b], who suggest that wintertime convection may play the key role in the formation and regeneration of what they refer to as a pycnocline lens in the Norwegian Sea. Figure 1 reveals an extremum in the sea surface height along with a closed isohaline of what we will argue is a permanent eddy in the Lofoten Basin.

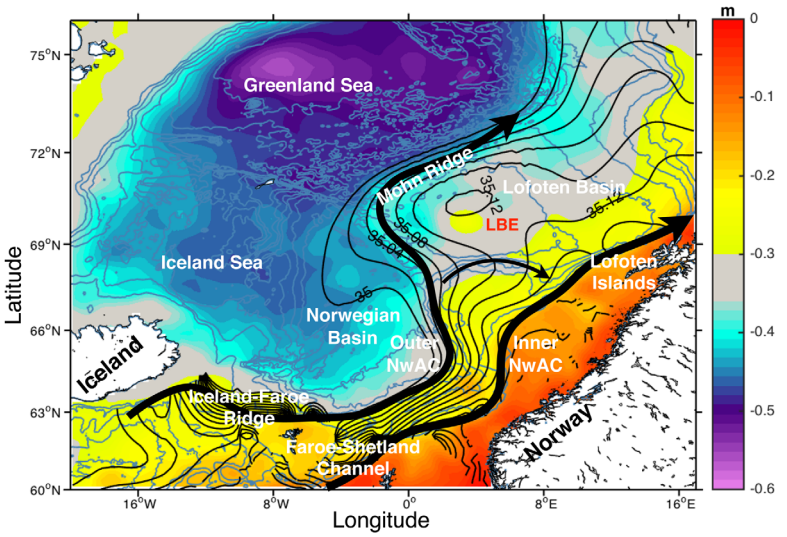

Figure 1. Map of the Nordic Seas showing the two principal pathways of warm Atlantic water (black arrows), bathymetry (blue contours with a spacing of 500 m), time-averaged dynamic topography (shading), and salinity at 300 m depth from the high-resolution World Ocean Atlas 2013 (black contours). The Nordic Seas include the Iceland Sea, the Greenland Sea, and the Norwegian Sea with its two subbasins the Norwegian Basin and Lofoten Basin with its the large horizontal extent of Atlantic water. The Lofoten Basin deepens from east to west and exceeds 3000 m in the western half.

As part of a larger effort to study, the thermocline circulation of the Lofoten Basin using a combination of moorings, hydrography, and RAFOS floats, a detailed survey of this eddy was conducted in July 2010. Using a vessel-mounted 75 kHz ADCP, a 14–16 km diameter core was found to be in solid body rotation with a relative vorticity close to its theoretical maximum magnitude $-f$ (the local Coriolis parameter). A hydrographic cast at the center showed that the core temperature was very close to adiabatic to depths greater than 1000 m [*Søiland and Rossby*, 2013]. RAFOS floats were deployed in this core and remained trapped in the eddy for up to 9 months. This finding of such a rapidly spinning core led to subsequent surveys in each of the following summers 2011–2015. This paper reports on these surveys and concludes on the basis of these, a concomitant analysis of altimetric data of the region, and a review of historical hydrographic data. We highlight that this eddy is not only a stable, persistent feature of the Lofoten Basin, but also given the way that it is maintained by the continual supply of eddies from the Lofoten escarpment quite possibly has existed continuously not merely for the last half century for which we have data, but quite possibly on millennial time scales, and as such plays a key role in maintaining the baroclinic structure of much of the Lofoten Basin. We will call this eddy the Lofoten Basin Eddy (LBE) in what follows (cf. Figure 1). The next section (2) briefly recapitulates the shipboard and satellite methods used. We then report our shipboard and altimetric findings in section 3, which are then discussed in section 4. A summary and conclusions end the paper.

2. Data and Methodology

2.1. Estimation of Ship-Measured Parameters

A total of five shipboard LBE surveys were conducted in 2010, 2012, 2013, 2014, and 2015. In addition, an anticyclonic eddy, here termed a Lofoten Eddy (LE), was surveyed in 2011. These include 75 kHz Vessel Mount ADCP transects to 600–800 m depth and hydrographic casts at selected sites. The ADCP sections are particularly effective at determining eddy strength in terms of dynamic height anomalies and eddy potential and kinetic energy budgets. The starting point is the momentum equation for curved flow (gradient wind) that gives us the dynamic height anomaly $\Phi(=-gz)$:

$$-\frac{v^2}{r}-fv=-\frac{1}{\rho}\frac{\partial p}{\partial r}=\frac{\partial \Phi}{\partial r}, \tag{1}$$

where the cyclostrophic and Coriolis terms on the left hand side are known. Integrating equation (1) radially at various depths gives us a cross section of Φ. The total eddy potential (TPE) and kinetic energy (TKE) integrals are obtained from a volume integral of Φ and velocity, respectively, assuming radial symmetry:

$$TPE = \int \left[\int \rho \Delta \Phi dz \right] 2\pi r dr \tag{2}$$

and

$$TKE = \int \left[\int \frac{\rho}{2} v^2 dz \right] 2\pi r dr. \tag{3}$$

The inner integral is taken from the surface to a common maximum depth of the observations (500 m) and the outer integral from the center out to 60 km. This distance captures the full horizontal extent of the eddy rather well. However, due to the deep velocity maximum in the LBE, it is an underestimate of TKE. The vertically averaged dynamic height is shifted so it goes through zero at 60 km radius to only capture the eddy and avoid contributions from the surrounding field. The relative vorticity can be obtained directly from the velocity field:

$$\zeta = \frac{v}{r} + \frac{\partial v}{\partial r}. \tag{4}$$

Although this expression becomes ill-defined where the section passes the center ($r \sim 0$), one can still obtain a vertical profile of relative vorticity at the center by assuming it rotates as a solid body and fitting a quadratic stream function (whose Laplacian is a constant) to the velocity vectors at each depth out to the radius of maximum solid body rotation, typically around 7–8 km. The quality of the estimate will vary depending upon the number of vectors available. The reader is referred to *Søiland and Rossby* [2013] for a further discussion of the data processing procedures employed here.

As has been observed in other studies of coherent eddies, RAFOS floats deployed in the core of such features may remain trapped in it for many months [*Rossby*, 1988; *Armi et al*., 1989]. We use the same approach here giving us valuable information on the position and strength of the LBE as a function of time. The orbital trajectories give us an effective measure of where the LBE is located at any given time, while the orbiting or looping period gives relative vorticity of the core while orbiting at small radii.

2.2. Satellite Altimetry and the RAFOS Float

Daily maps of Sea Surface Height (SSH) derived from all available satellites (provided by AVISO) give us information on dynamic topography [*Pascual et al*., 2006; *Rio et al*., 2011] and how it varies spatially on 1/4° grid and temporally over the 1993–2014 time interval. *Volkov and Pujol* [2012] show that altimetry can be successfully used to study the sea-surface height variability and circulation of the Nordic Seas. In order to determine LBE movement during the 22 years of altimetric coverage, we first used knowledge of the LBE's position during the 9 months it was tracked with a RAFOS float to develop an altimetric procedure that best reproduces the position of the Eddy (supporting information animation S1 confirms the excellent daily consistency between the altimetry and float-estimated position).

2.3. Hydrography

We use the high-resolution regional (Nordic and Barents Seas) hydrographic data set produced by the National Oceanographic Data Center and compiled using 37 different sources of data [*Korablev et al*., 2014; *Seidov et al*., 2015]. The data are compiled on a 0.25° ×0.25° grid with one map per month. The generally high density of hydrographic data in the Nordic Seas (more than 10 stations within each quarter-degree grid box for the annual period) in combination with a sophisticated objective analysis method [*Troupin et al*., 2012] has resulted in a reconstruction of the hydrography on a quarter-degree grid with relatively high confidence [*Seidov et al*., 2015]. In fact, using this data set, *Chafik et al*. [2015] detected and traced temperature anomalies both into the Lofoten Basin and towards the Fram Strait. In this study, we use six decadal averages (1950s, 1960s, 1970s, 1980s, 1990s, and 2000s) of the temperature field at 800 m depth within the deeper part of the Lofoten Basin to highlight the permanency of the LBE.

3. Results

3.1. ADCP/CTD Surveys

The unexpectedly well-defined eddy that was surveyed in July 2010 led to an effort to revisit the area as regularly as possible. Thus we now have five surveys of the LBE and one survey of a LE. We used the VM-

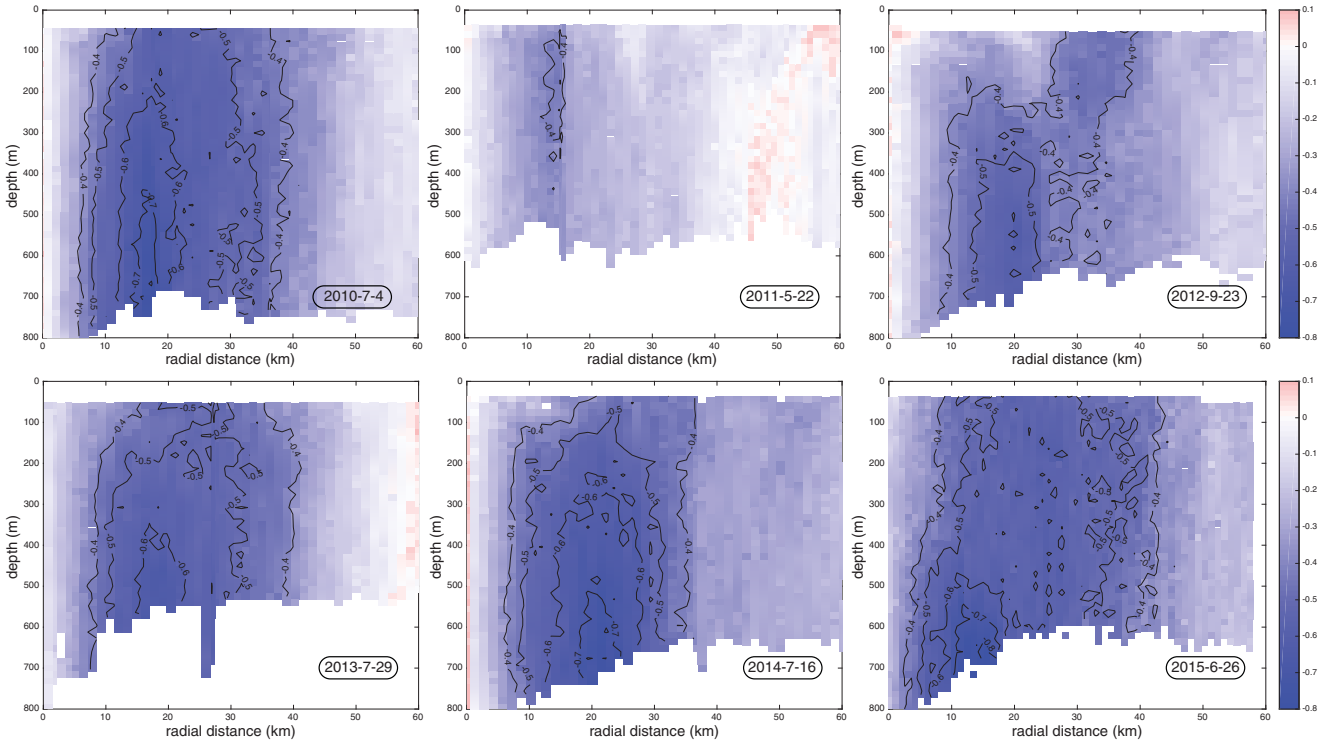

Figure 2. Radial cross sections of azimuthal velocity for the six surveys. The velocity maximum is not at the surface, but near or below the maximum reach of the ADCP. The eddy in 2011 is weaker and smaller both horizontally and vertically.

ADCP to determine the center of the LBE and conducted radial surveys. The visits are brief, but long enough to obtain radial ADCP sections and a few CTDs to characterize the density field; here we focus principally on the velocity field to determine the size and strength of the eddy at each visit. Figure 2 shows a radial-vertical section of velocity for each of the five LBE and the 2011 survey of the LE, organized for easy comparison. The five LBE panels (years 2010, 2012–2015) show clearly that the velocity maximum is not close to the surface, but near the maximum reach of the ADCP. The LE surveyed in 2011 is notably weaker and smaller both horizontally and vertically and the velocity maximum is in the upper few hundred meters.

As a reference for satellite altimetry, we show radial profiles of dynamic height anomaly at 36 m depth in Figure 3. To quantify the strength of the LBE at the surface, we also fit a Gaussian function to the central part of each of these in the expectation that the rapidly spinning core is self-defining, and independent of the eddy field outside. It is noteworthy that the advantage of the Gaussian fit is twofold: it is an effective way to show that the internal structure of the LBE is robust, and it immediately gives us its characteristic scale. This is the amplitude an altimeter would on average observe. It is not the maximum strength of the LBE, which increases a few more dyn. cm with increasing depth and reaches a maximum near or perhaps beyond the reach of the 75 kHz ADCP (700–800 m).

The size and strength of the LBE and LE from the six surveys are given in Figure 4. What emerges from these six surveys are a comparative uniformity of size and amplitude from year-to-year, with year 2011 being an exception, which although not much smaller in radius is noticeably weaker in TPE and TKE. These integrals are well-behaved in the center of the eddy but can become erratic at large radii so some judgment must be exercised about where to stop the integration. Nonetheless, it is striking how stable the TPE/TKE ratio is. Use of the Gaussian function gives an effective tool to show that the radial scale of the LBE is conspicuously stable (or invariant) from year to year. Even the LE is quite similar in scale albeit noticeably weaker in strength. This applies to both its velocity structure (a) and heat content (g), which were obtained by entirely different means. The most invariant aspect of the LBE lies perhaps in its peak relative vorticity, close to $-f$. If the scale of the LBE is constant, this implies that its dynamic height maximum at depth is constant. Since ζ decreases toward the surface (not shown here, but see e.g., *Søiland and Rossby* [2013]), this also means that SSH may be more variable.

Another integral measure of eddy strength that will prove quite useful in the discussion is excess Heat Content (HC) due to the substantial downward displacement of the main thermocline in the LBE [*Søiland and*

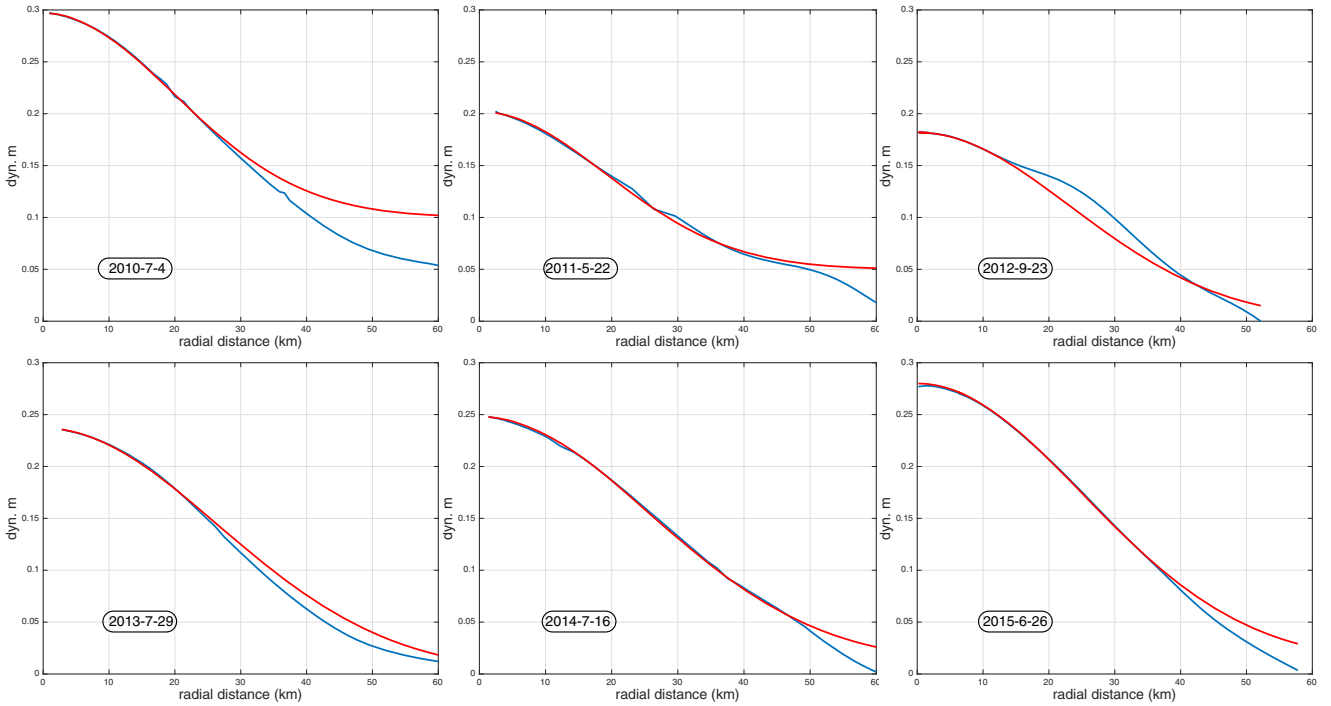

Figure 3. Radial distribution of dynamic height for each of the surveys. The blue curves are computed from azimuthal velocity at 36 m depth and the red curve represents a Gaussian fit to the blue curve for radial distances <40 km.

Rossby, 2013]. In Figure 5, we plot mean temperature from the surface to H = 1500 m from each of the surveys as a function of distance from the center. To facilitate estimating total heat content, we fit a Gaussian curve to the temperatures and then integrate radially:

$$HC = \rho C_p H \int_0^\infty \Delta T e^{-r^2/R^2} 2\pi r dr = \rho C_p H \Delta T H \pi R^2, \quad (5)$$

where R is the radial scale and ΔT (the vertically averaged temperature anomaly) the amplitude of the fit (R, ΔT, and HC values are also shown in Figure 4). Again, we see that the LE in 2011 was notably weaker than the LBE in other years. At the time of the survey, it was clear this was not the LBE, but an eddy originating from the Lofoten escarpment. Its thermocline depth was much shallower and the maximum swirl speed was found at a shallow depth compared to the LBE surveyed in 2010. This is confirmed by an altimetric view of sea level and surface geostrophic velocities at the time of the 2011 eddy survey: the LE sits close, but to the east of where the LBE normally is, and the LBE at the time is unusually far off to the northwest as shown in Figure 6.

3.2. LBE Dynamic Height From Altimetry and Hydrography

We begin with an assessment of altimetric tracking of the LBE during the 9 month period we knew exactly where it was thanks to a RAFOS float orbiting its core. To show that there is good consistency between the float position and LBE as viewed from altimetry during the entire 9 month period (cf. supporting information animation that show that this is true even on daily basis), we grouped the ADT maps into monthly means. The RAFOS float track was low-pass filtered at 8 days thereby removing the orbital movement within the eddy. The resulting track was then averaged for the same months as the ADT fields and plotted on the same map as shown in Figure 7. The agreement between the two is quite good. The scale is the same such that the color change represents a seasonal range from a maximum in September–October to a minimum in March. These monthly means have at least two and sometimes three contours (0.05 dyn. m) enclosing the maximum. Further use of the 9 month float position, Figure 8, highlights that the LBE drift in a cyclonic manner in the deepest part of the Lofoten Basin bounded by the 3250 m depth contours. The cyclonic drift of the LBE based on observations was reported earlier by *Ivanov and Korablev* [1995b] and implied by an altimetry-based eddy propagation pattern presented by *Volkov et al.* [2015].

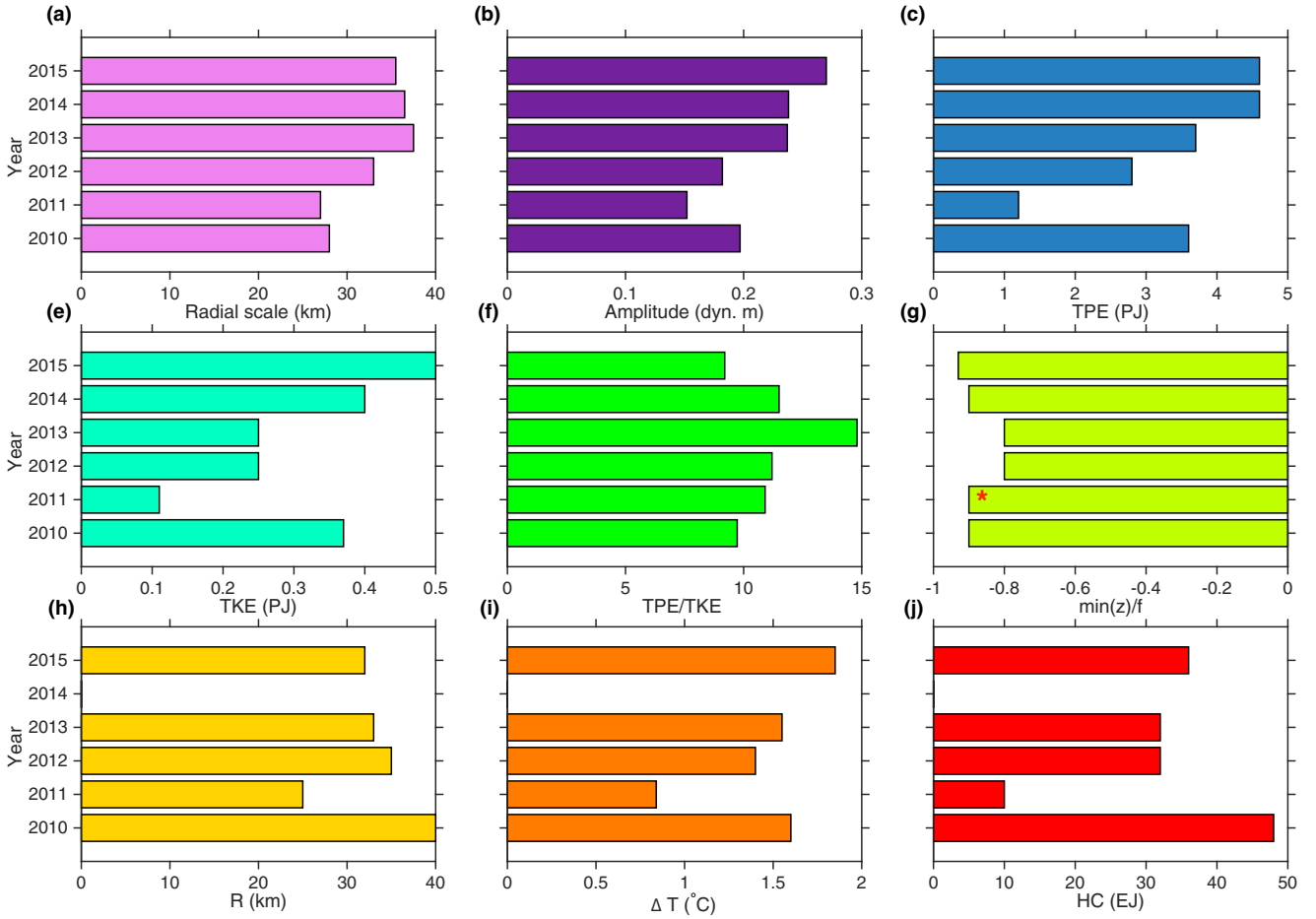

Figure 4. Summary of LBE characteristics from the six ADCP surveys. (a–b) Radial scale and amplitude based on a Gaussian fit to dynamic height anomaly of central part of eddy at 36 m depth (3), (c–d) TPE and TKE according to equations (2) and (3), (e) The TPE/TKE ratio, (f) vertical extremum of relative vorticity in the core of the eddy normalized by the local Coriolis parameter, (g–i) R, ΔT, and Heat Content (HC) (in Exa-Joules). The missing estimates of 2014 (Figures 4g–4i) are due to winch problems limited casts to 1000 m during that year. The red star in the 2011 relative vorticity (Figure 4f) indicate very rough estimate.

Given the above validation of the SSH method to track the LBE, we use the same procedure to construct a probability distribution of position of the LBE center based on the extremum in SSH for the 22 years (Figure 9a), and we also show how this extremum has varied between 1993 and 2014 (Figure 9b). Its wandering is rather limited such that less than 50% of the time the LBE will be outside a 80 km north-south × 95 km east-west domain. The bathymetric contours show how this probability coincides with the deepest part of the Lofoten Basin defined by the 3220 m contour. The right plot shows the peak SSH found within the same search area as a function of time. One sees clearly the seasonal rhythm with maxima/minima in late summer/winter. In spite of variability on multiple time-scales (seasonal, interannual, trend), the local maximum in SSH is a good metric for the center position of the LBE. There are some striking variations, the causes of which will require further study—such as the overall lower SSH before 1996, which coincides with a period of strong North Atlantic Oscillation [*Woolf et al*., 2003; *Chafik et al*., 2015]. The interannual variability of the peaks will depend upon a combination of factors including the heat loss patterns over the western Lofoten Basin, and sea level variations due to the state of the surrounding eddy field. The LBE sea level rise is about ∼5 mm per year if considering the 1993–2014 period, however, it is reduced to ∼2 mm per year between 1996 and 2014. This increase is likely due to the warming of the Nordic Seas [*Skagseth and Mork*, 2012; *Mork et al*., 2014], and the numbers are consistent with global sea level rise [*Chen et al*., 2014].

On longer time scales, hydrographic stations are our only source of information. Although the stations are spottier, the objectively analyzed hydrographic data on a 0.25° × 0.25° grid analyzed [*Korablev et al*., 2014] reveal the existence of the LBE since the 1950s. One sees this both in terms of excess temperature at depth and especially in greater temperature variability coinciding with time-mean SSH, Figure 10. (Note, however,

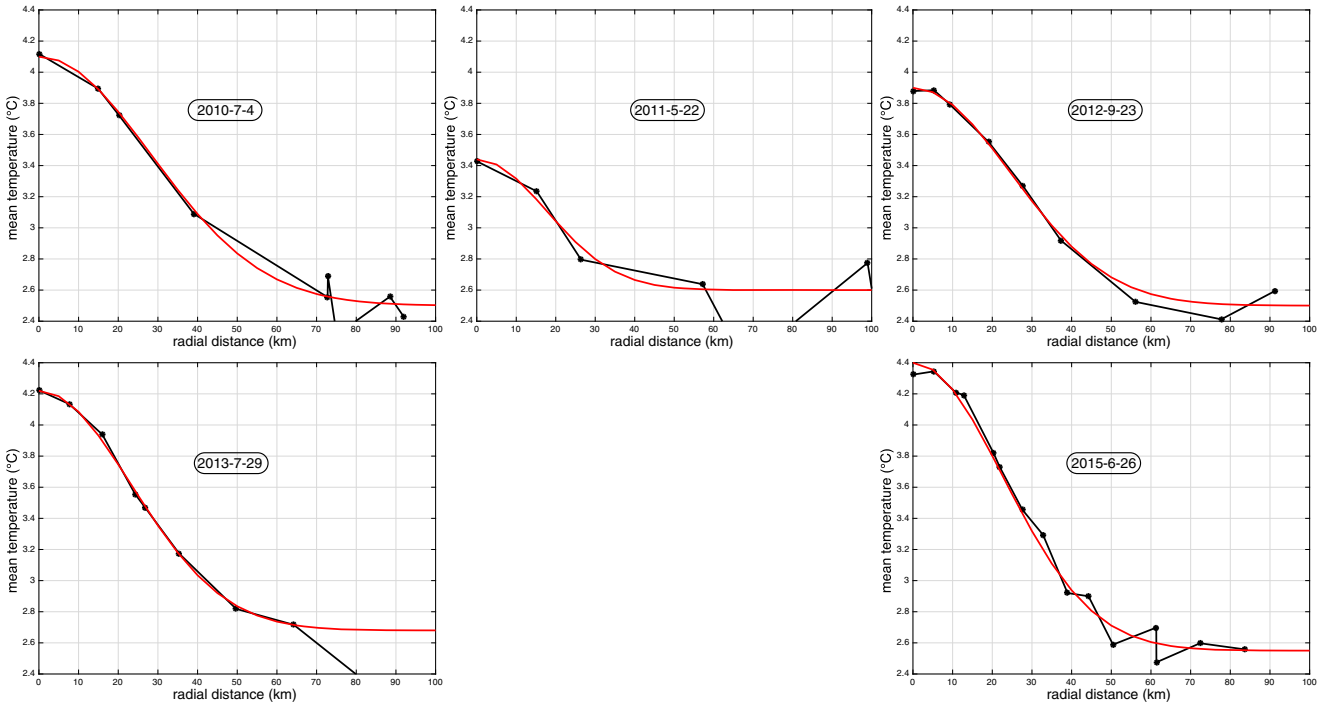

Figure 5. Radial distribution of 0–1500 mean temperature from all hydrostations (blue lines). The red curve is a Gaussian fit to the stations with emphasis on stations in/near the core of the eddy. Note that there is no HC for 2014 because the CTDs were limited to 1000 m.

when the station data is denser, the location of LBE core from altimetry and hydrography is more consistent). In an overall sense, the decadal standard deviation of temperature of the LBE core varies between 1.1–1.3°C, except for the 1990–1999 where the maximum standard deviation of the LBE core displayed a value of 0.9°C.

4. Discussion

The above data sets and surveys strongly suggest that the LBE is a permanent feature of the Lofoten Basin. While the five LBE surveys indicate some variability, the ∼15% scatter in dynamic height anomaly at the surface, ∼7% scatter in peak relative vorticity, and 20% in TPE suggest a dynamical structure with considerable robustness (Figure 4). The higher variability in TPE and heat content (HC), both of which are single radial

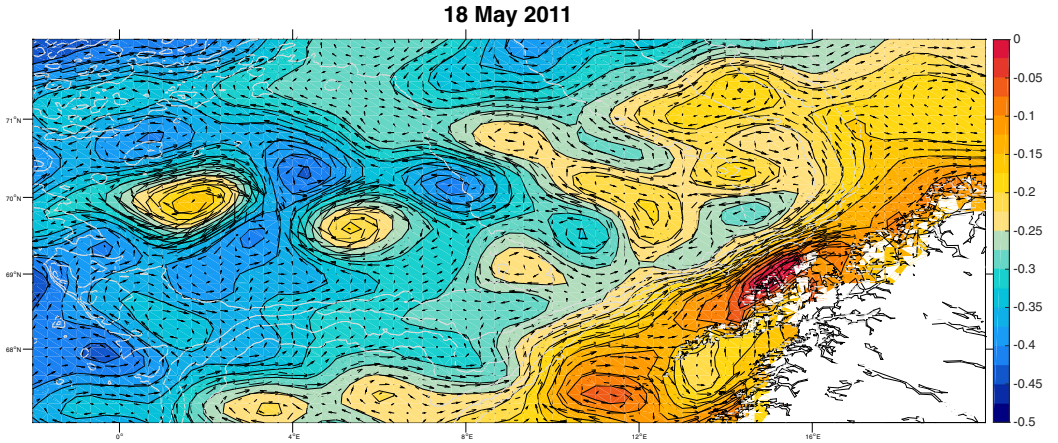

Figure 6. SSH for the Lofoten Basin at the time of the LBE survey in 2011. Note the LBE farther west than usual and the LE close to the normal position of the LBE. The gray contours indicate the bathymetry with a spacing of 500 m.

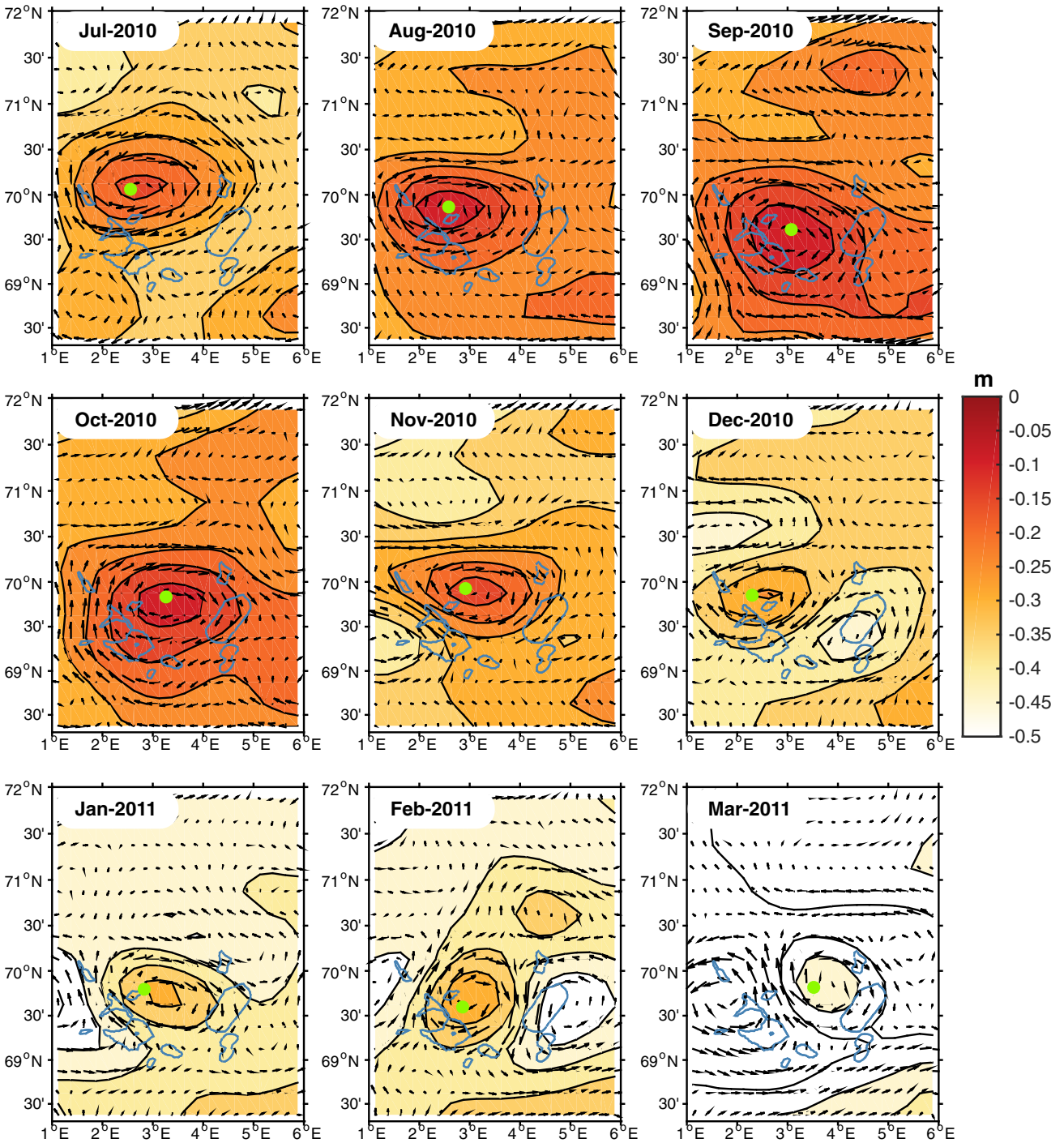

Figure 7. Nine monthly averages of SSH in the western Lofoten Basin. The change in color represents the seasonal variation. Each mean field has a maximum near 70°N 3°E and for each the mean position of the LBE according to the RAFOS float is indicated by the green dot. The bathymetric contour is the 3250 m, where the LBE seems to be trapped.

integrals, very likely reflects variations in the eddy field present on that line. This is evident in Figure 2, which shows greater variability of azimuthal velocity at larger radii than near the center of the eddy. While there are no wintertime surveys, the sustained orbital motion of a RAFOS float for 9 months clearly suggests uninterrupted continuity through the winter months.

Another measure of eddy stability comes from the temperature profiles taken at the center of the eddy on each survey (Figure 11). All five LBE surveys exhibit very small temperature changes (<0.5°C) from the

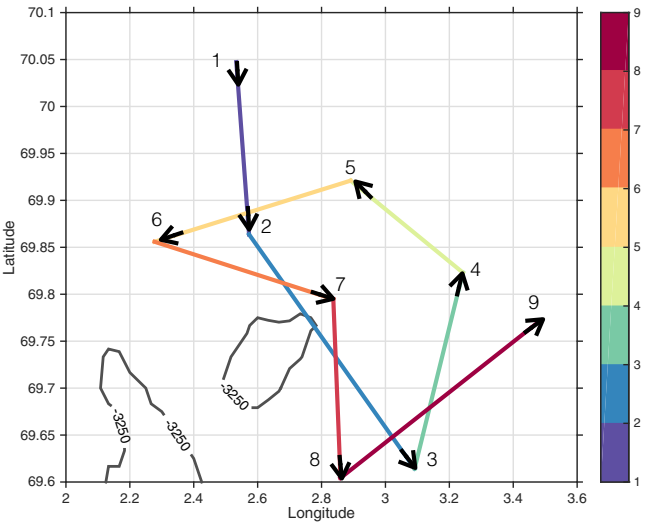

Figure 8. The monthly position of the RAFOS float during the 9 months (numbers) as it was trapped by the LBE. The arrows indicate a cyclonic movement of the float/LBE during this period.

seasonal thermocline to more than ~1000 m depth. All the profiles have a depth interval with close to adiabatic conditions, and in 2010 and 2012 this interval is about 600–800 m. It seems rather remarkable that such conditions would still apply up to 6 months after the cessation of intense wintertime heat loss driving deep and possibly penetrative convection, Figure 11. *Ivanov and Korablev* [1995a,b] suggested that such convection might play a key role in the "rejuvenation" of the LBE through the deepening of the underlying pycnocline thereby increasing the radial baroclinicity and thus lead to an increased angular velocity. Possible evidence for such an increase can be seen in the nine month RAFOS float record in *Søiland and Rossby* [2013].

It is now well established that the required heat comes from the Lofoten eddies (LEs) that break away from the NwAC and drift west towards the LBE [*Köhl*, 2007; *Rossby et al*., 2009b; *Søiland and Rossby*, 2013; *Raj et al*., 2015; *Volkov et al*., 2015] thereby defining what might be called a "corridor" from the Lofoten escarpment to the LBE. *Raj et al*. [2015] estimated from the 1995–2010 AVISO record that 110 LEs were spawned; a production rate of one LE every 2 months. The LEs are transported westward and some of them are absorbed by the LBE and thus contribute to the maintenance of the LBE. However, since the LEs are comparable in size (but not as deep) to the LBE, only a small fraction of these or the water transported by these can be absorbed by the LBE considering that the LBE remains fairly constant in size and strength. The rest must instead be dispersed to the surrounding waters. This would explain the generally deep thermocline in the general vicinity of the LBE. The bimonthly supply of ~10 EJ (EJ is exa Joule or 10^{18}J) each tells us that over a 1 year period about 60 EJ is brought into the region of the LBE. The circular area required to lose this heat to the atmosphere assuming an annual average of 80 W/m^2 [*Richards and Straneo*, 2015] has a radius of 87 km; close to 2 times the size of the LBE. However, given that the LBE has a deep mixed layer and can maintain a high heat loss throughout the winter the effective heat loss rate may be greater. This areal

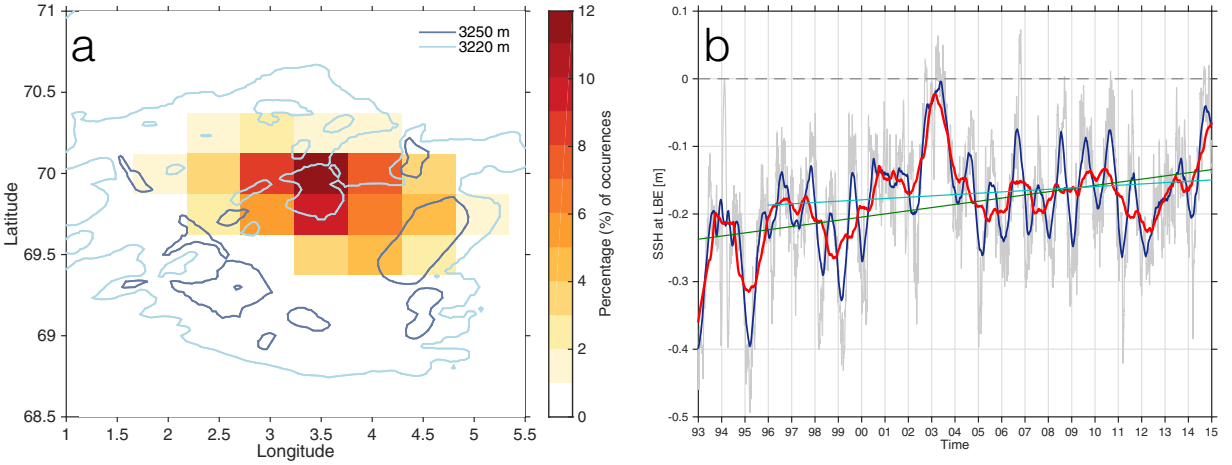

Figure 9. (a) The 2-D probability distribution of the LBE center obtained from the daily 22 year period and expressed in percentage of occurrences (shading). The heavy and light bathymetric contours (3250 and 3220 m) indicate the deepest waters in the Lofoten Basin. (b) Time series of the SSH corresponding to the LBE center (extremum in the same search area as in Figure 9a). Gray are the daily samples, low-pass filtered to 6 months (blue), and 1 year (red). The green trend line shows an estimate of sea level rise at the LBE by ~5 mm/yr (1993–2014), while the turquoise is ~2 mm/yr (1996–2014). The global mean sea level has not been subtracted from the local trends.

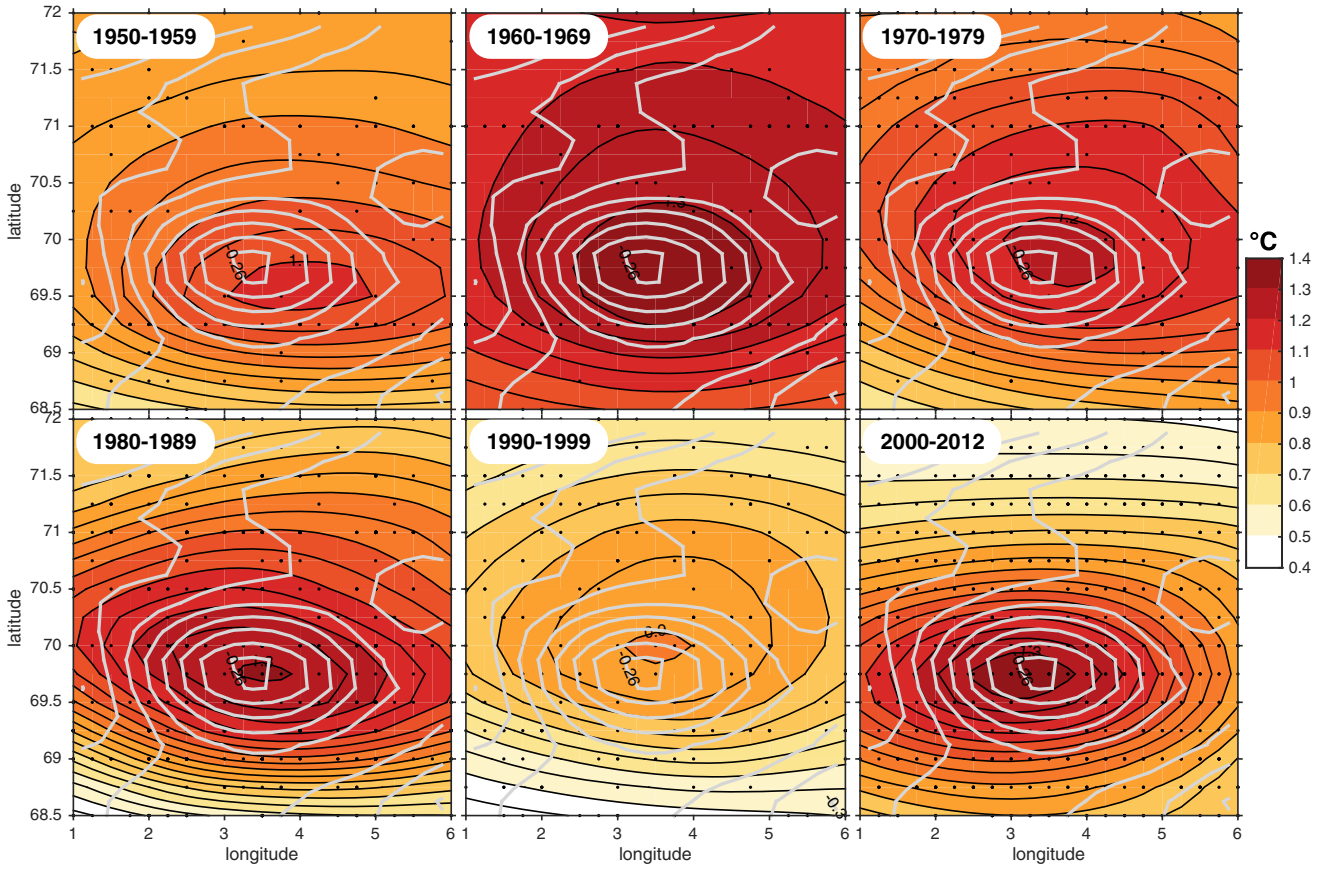

Figure 10. Standard deviation of temperature at 800 m in the western Lofoten Basin for the last 6 decades (shading); in all cases with the maximum coinciding with the mean position of the LBE inferred from the time-mean SSH. The interdecadal variability may reflect decadal climate change. The dots indicate the stations used for the objective analysis during each decade [*Korablev et al.*, 2014].

estimate depends upon having more accurate knowledge of wintertime heat loss patterns; existing reanalyses of ocean-atmosphere heat exchange do not have this spatial resolution. Also, since the eddy remains relatively constant in size, it may also lose heat as it loses water to the surroundings.

The Atlantic water flowing toward the Arctic along the Lofoten Escarpment is expelled partially as discrete LEs and partially through eddy exchange processes. The westward flux of heat and salt by the LEs together with the permanent LBE play a central role in maintaining the large pool of warm water of especially the western Lofoten Basin. We do not have accurate in situ measurements of transport by the NwAC up and downstream of the Lofoten Escarpment, but estimates from AVISO [*Chafik et al.*, 2015] suggest a decrease from ~1.5–2 Sv (67–69°N) to ~0.5–1 Sv (70–72°N). This is comparable to the volume flux associated with the transit of the LEs from the escarpment toward the LBE: the volume of the LE $\sim \pi \times 25^2$ km^2 $\times$ 1000 m deep (say) divided by 60 days $\sim$ 0.4 Sv, but neither of these estimates are accurate enough for direction comparison. There is good evidence that the NwAC leaks into the Lofoten Basin [cf. *Chafik et al.*, 2015]. First, we have the dispersion of RAFOS floats from the current *Rossby et al.* [2009b]. Of 14 floats in the NwAC that reached or continued beyond the Lofoten Basin roughly half of them were expelled into the basin. Second, *Koszalka et al.* [2011, 2013] note the high loss of surface drifters in this same region (off the Lofoten Escarpment), but they were not trapped in LEs.

Interestingly the Lofoten escarpment and the Lofoten Basin morphology plays a major role in modifying the properties of the Atlantic water flowing into the Barents Sea and Fram Strait and ultimately into the Arctic Ocean. *Volkov et al.* [2015] show that in order to achieve a realistic hydrographic structure in the Lofoten Basin that includes the LBE a very high-resolution model (4 km $\times$ 4 km) is required. Experiments with coarser resolution such as 18 km does not result in a LBE. This begs the question how well climate models

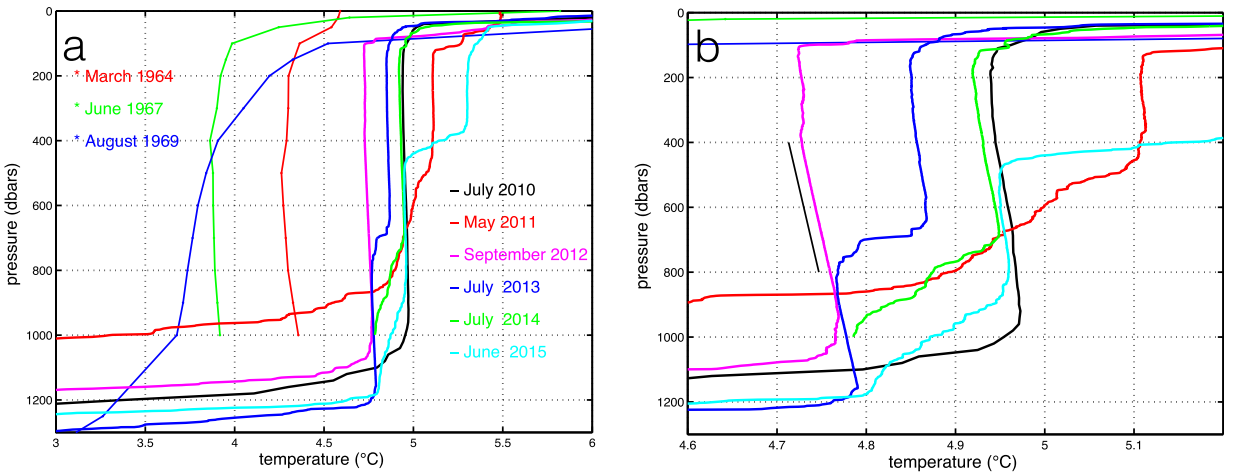

Figure 11. (a) Profiles of temperature at the center of the eddies for each of the six surveys, five LBE, and one LE surveys. The thin profiles are from the 1960s. They are colder reflecting the colder conditions at the time. (b) A closer look at the center profiles from the six surveys from the recent years with the adiabatic temperature gradient included (thin black line).

are resolving the lateral fluxes and pooling and deepening of Atlantic water in the Lofoten Basin; aspects of great importance for the ocean heat transport to the Arctic, but also for the meridional overturning circulation [*Richards and Straneo*, 2015].

5. Summary and Conclusions

The purpose of this study has been to characterize the LBE spatially and temporally. In recent years, several studies have identified the area around 69–70°N 3–4°E as one with a deepened thermocline, a local sea level maximum, and high eddy activity. Our results reinforce that these extrema are in large measure due to a permanent structure, the LBE, wandering about in a topographically limited region. The five surveys of the LBE clearly reveal a well-defined coherent structure with an anticyclonically rotating core with a relative vorticity $\sim$-0.85 $\times$ the local Coriolis parameter, i.e., not much less than its -1 theoretical limit. The first 9 months of a float trajectory, while it was still trapped in the eddy, reveal a stably rotating core with no disruption in its orbital motion. This is significant for it indicates that the core of the LBE remains quite stable, almost immune or isolated from its interactions with the surrounding waters.

The enormous reservoir of heat stored in the LBE is clearly maintained by a continual supply of eddies being shed by the Norwegian Atlantic Current where it flows past the Lofoten Escarpment. These eddies drift west toward the LBE. By good fortune, one such eddy was surveyed and assuming it is typical in size and heat content—it is clear that the LBE cannot absorb all these eddies. Instead, a fraction of their water will be entrained or wrapped around the LBE and the rest will be dispersed through meso and submesoscale processes to the surrounding waters. Of course, some LEs may collide with others or drift in other directions. Evidence for this lies in the generally deeper isopycnals in the western part of the Lofoten Basin. Thus, the large pool of heat in the Lofoten Basin compared to the Norwegian Basin farther south is a consequence of warm eddies being expelled where the Norwegian Atlantic Current flows past the steep Lofoten Escarpment. Given that the production of these eddies is an unceasing process, and the documentary evidence for a permanent LBE over the last 50–60 years from a combination of hydrography and altimetry, it seems plausible that the LBE is, despite its small size, a permanent feature of the circulation of the Nordic Seas.

Acknowledgments
We thank the reviewers for the helpful and constructive suggestions. We are grateful to the Institute of Marine Research for providing ship time for the surveys. We also thank the Bjerknes Centre for Climate Research for its support. Léon Chafik is supported by a grant from the NOAA Jason altimetry program. The satellite-altimetry data set, denoted SSALTO/DUACS (multimission ground Segment for ALTimetry, Orbitography, and precise localization/Developing Use of Altimetry for Climate Studies), was obtained courtesy of the French archive AVISO (Archiving, Validation and Interpretation of Satellite Oceanographic Data, http://www.aviso.oceanobs.com).

References

Andersson, M., K. A. Orvik, J. H. LaCasce, I. Koszalka, and C. Mauritzen (2011), Variability of the Norwegian Atlantic Current and associated eddy field from surface drifters, *J. Geophys. Res.*, *116*, C08032, doi:10.1029/2011JC007078.

Armi, L., D. Hebert, N. Oakey, J. F. Price, P. L. Richardson, H. T. Rossby, and B. Ruddick (1989), Two years in the life of a Mediterranean Salt lens, *J. Phys. Oceanogr.*, *19*(3), 354–370.

Björk, G., B. Gustafsson, and A. Stigebrandt (2001), Upper layer circulation of the Nordic seas as inferred from the spatial distribution of heat and freshwater content and potential energy, *Polar Res.*, *20*(2), 161–168.

Chafik, L., J. Nilsson, Ø. Skagseth, and P. Lundberg (2015), On the flow of Atlantic water and temperature anomalies in the Nordic seas toward the arctic ocean, *J. Geophys. Res. Oceans*, *120*, 7897–7918, doi:10.1002/2015JC011012.

Chen, X., Y. Feng, and N. E. Huang (2014), Global sea level trend during 1993–2012, *Global Planet. Change*, *112*, 26–32, doi:10.1016/j.gloplacha.2013.11.001.
Helland-Hansen, B., and F. Nansen (1909), The Norwegian Sea: Its physical oceanography based upon the Norwegian researches 1900–1904, Part 1, *Rep. Norw. Fish. Mar. Invest.*, *2*, 390 pp.
Ivanov, V. V., and A. A. Korablev (1995a), Formation and regeneration of the pycnocline lens in the Norwegian sea, *Russ. Meteorol. Hydrol.*, *9*, 62–69.
Ivanov, V. V., and A. A. Korablev (1995b), Dynamics of an intrapycnocline lens in the Norwegian sea, *Russ. Meteorol. Hydrol.*, *10*, 32–37.
Köhl, A. (2007), Generation and stability of a quasi-permanent vortex in the Lofoten basin, *J. Phys. Oceanogr.*, *37*(11), 2637–2651, doi:10.1175/2007JPO3694.1.
Korablev, A. A., A. Smirnov, and O. K. Baranova (2014), Climatological Atlas of the Nordic Seas and Northern North Atlantic, in NOAA Atlas NESDIS 77, edited by D. Seidov and A. R. Parsons, 122 pp., doi:10.7289/V5K64G16.
Koszalka, I., J. H. LaCasce, M. Andersson, K. A. Orvik, and C. Mauritzen (2011), Surface circulation in the Nordic Seas from clustered drifters, *Deep Sea Res., Part I*, *58*(4), 468–485, doi:10.1016/j.dsr.2011.01.007.
Koszalka, I., J. H. LaCasce, and C. Mauritzen (2013), In pursuit of anomalies: Analyzing the poleward transport of Atlantic Water with surface drifters, *Deep Sea Res., Part II*, *85*, 96–108, doi:10.1016/j.dsr2.2012.07.035.
Mork, K. A., Ø. Skagseth, V. Ivshin, V. Ozhigin, S. L. Hughes, and H. Valdimarsson (2014), Advective and atmospheric forced changes in heat and fresh water content in the Norwegian Sea, 1951–2010, *Geophys. Res. Lett.*, *41*, 6221–6228, doi:10.1002/2014GL061038.
Orvik, K. A., and P. Niiler (2002), Major pathways of Atlantic water in the northern North Atlantic and Nordic Seas toward Arctic, *Geophys. Res. Lett.*, *29*(19), 1896, doi:10.1029/2002GL015002.
Pascual, A., Y. Faugère, G. Larnicol, and P.-Y. Le Traon (2006), Improved description of the ocean mesoscale variability by combining four satellite altimeters, *Geophys. Res. Lett.*, *33*, L02611, doi:10.1029/2005GL024633.
Poulain, P. M., A. Warn-Varnas, and P. P. Niiler (1996), Near-surface circulation of the Nordic seas as measured by Lagrangian drifters, *J. Geophys. Res.*, *101*(C8), 18,237–18,258, doi:10.1029/96JC00506.
Raj, R. P., L. Chafik, J. E. Ø. Nilsen, T. Eldevik, and I. Halo (2015), The Lofoten vortex of the Nordic seas, *Deep Sea Res., Part I*, *96*, 1–14, doi:10.1016/j.dsr.2014.10.011.
Richards, C. G., and F. Straneo (2015), Observations of water mass transformation and eddies in the Lofoten Basin of the Nordic seas, *J. Phys. Oceanogr.*, *45*(6), 1735–1756, doi:10.1175/JPO-D-14-0238.1.
Rio, M. H., S. Guinehut, and G. Larnicol (2011), New CNES-CLS09 global mean dynamic topography computed from the combination of GRACE data, altimetry, and in situ measurements, *J. Geophys. Res.*, *116*, C07018, doi:10.1029/2010JC006505.
Rossby, T. (1988), Five drifters in a Mediterranean salt lens, *Deep Sea Res., Part A*, *35*(9), 1653–1663, doi:10.1016/0198-0149(88) 90108-2.
Rossby, T., V. Ozhigin, V. Ivshin, and S. Bacon (2009a), An isopycnal view of the Nordic Seas hydrography with focus on properties of the Lofoten Basin, *Deep Sea Res., Part I*, *56*(11), 1955–1971, doi:10.1016/j.dsr.2009.07. 005.
Rossby, T., M. D. Prater, and H. Søiland (2009b), Pathways of inflow and dispersion of warm waters in the Nordic Seas, *J. Geophys. Res.*, *114*, C04011, doi:10.1029/2008JC005073.
Seidov, D., et al. (2015), Oceanography north of 60°N from World Ocean Database, *Prog. Oceanogr.*, *132*, 153–173, doi:10.1016/j.pocean.2014.02.003.
Skagseth, Ø., and K. A. Mork (2012), Heat content in the Norwegian Sea, 1995–2010, *ICES J. Mar. Sci.*, *69*, 826–832.
Skagseth, Ø., K. A. Orvik, and T. Furevik (2004), Coherent variability of the Norwegian Atlantic Slope Current derived from TOPEX/ERS altimeter data, *Geophys. Res. Lett.*, *31*, L14304, doi:10.1029/2004GL020057.
Søiland, H., and T. Rossby (2013), On the structure of the Lofoten Basin Eddy, *J. Geophys. Res. Oceans*, *118*, 4201–4212, doi:10.1002/jgrc.20301.
Troupin, C., et al. (2012), Generation of analysis and consistent error fields using the Data Interpolating Variational Analysis (DIVA), *Ocean Modell.*, *52–53*, 90–101, doi:10.1016/j.ocemod.2012.05.002.
Volkov, D. L., and M. I. Pujol (2012), Quality assessment of a satellite altimetry data product in the Nordic, Barents, and Kara seas, *J. Geophys. Res.*, *117*, C03025, doi:10.1029/2011JC007557.
Volkov, D. L., T. V. Belonenko, and V. R. Foux (2013), Puzzling over the dynamics of the Lofoten Basin: A sub-Arctic hot spot of ocean variability, *Geophys. Res. Lett.*, *40*, 738–743, doi:10.1002/grl.50126.
Volkov, D. L., A. A. Kubryakov, and R. Lumpkin (2015), Formation and variability of the Lofoten basin vortex in a high-resolution ocean model, *Deep Sea Res., Part I*, *105*, 142–157, doi:10.1016/j.dsr.2015.09.001.
Woolf, D. K., A. G. P. Shaw, and M. N. Tsimplis (2003), The influence of the North Atlantic oscillation on sea-level variability in the North Atlantic region, *J. Atmos. Ocean Sci.*, *9*(4), 145–167, doi:10.1080/10236730310001633803.

Erratum

In the originally published version of this article, there are erroneous annotations in Figure 11a. The figure annotations has since been corrected, and this version may be considered the authoritative version of record.